0026-895X/04/6501-181–195$20.00
MOLECULAR PHARMACOLOGY
Copyright © 2004 The American Society for Pharmacology and Experimental Therapeutics
Mol Pharmacol 65:181–195, 2004

Vol. 65, No. 1
2759/1118438
Printed in U.S.A.

Examination of the Mechanism(s) Involved in Doxorubicin-Mediated Iron Accumulation in Ferritin: Studies Using Metabolic Inhibitors, Protein Synthesis Inhibitors, and Lysosomotropic Agents

J. C. Kwok and D. R. Richardson

Children's Cancer Institute Australia for Medical Research, Iron Metabolism and Chelation Program, Randwick, Sydney, New South Wales, Australia

Received June 23, 2003; accepted October 1, 2003

This article is available online at http://molpharm.aspetjournals.org

ABSTRACT

Anthracyclines are potent anticancer agents, but their use is limited by cardiotoxicity at high cumulative doses. The mechanisms involved in anthracycline-mediated cardiotoxicity are still poorly understood, but numerous investigations have indicated a role for iron in this process. Our previous studies using neoplastic and myocardial cells showed that anthracyclines inhibit iron mobilization from the iron storage protein, ferritin, resulting in marked accumulation of ferritin-iron. Although the process of ferritin-iron mobilization is little understood, catabolism of ferritin by lysosomes may be a likely mechanism. Because anthracyclines have been shown to accumulate in lysosomes, this latter organelle may be a potential target for these drugs. The present study demonstrated, using native polyacrylamide gel electrophoresis-^{59}Fe autoradiography, that ferritin-^{59}Fe mobilization is an energy-dependent process that also requires protein synthesis. Depression of lysosomal activity via the enzyme inhibitors E64d [(2*S*,3*S*)-*trans*-epoxysuccinyl-L-leucylamido-2-methylbutane ethyl ester] and leupeptin or the lysosomotropic agents ammonium chloride, chloroquine, and methylamine resulted in a 3- to 5-fold increase in ^{59}Fe-ferritin accumulation compared with control cells. In addition, the proteasome inhibitors *N*-benzoyloxycarbonyl (*Z*)-Leu-Leu-leucinal (MG132) and lactacystin also significantly increased ^{59}Fe-ferritin levels compared with control cells. These effects of lysosomotropic agents or inhibitors of lysosomal activity were comparable with that observed with the anthracycline doxorubicin. Collectively, our study indicates a role for lysosomes and proteasomes in ferritin-iron mobilization, and this pathway is dependent on metabolic energy and protein synthesis. Furthermore, the lysosome/proteasome pathway may be a novel anthracycline target, inhibiting iron mobilization from ferritin that is essential for vital iron-requiring processes such as DNA synthesis.

The clinical use of anthracyclines as a potent class of anticancer agents is greatly hindered by the development of cardiotoxicity at high cumulative doses (Gianni and Myers, 1992). However, the precise mechanisms by which anthracyclines cause cardiotoxicity are still poorly understood. Numerous investigations strongly support a role for iron in anthracycline-mediated cardiotoxicity (Gianni and Myers, 1992). Despite the ability of anthracyclines to avidly bind iron (Gianni and Myers, 1992), few studies have examined the effect of these drugs on cellular iron metabolism. The most comprehensive experiments to date have examined the effects of anthracyclines on the iron regulatory proteins (Minotti et al., 1998; Kotamraju et al., 2002; Kwok and Richardson, 2002a). The iron regulatory proteins are involved in post-translational regulation of molecules involved in iron metabolism, including ferritin and the transferrin receptor 1 (TfR1) (Kwok and Richardson, 2002b). Further studies examining the effect of anthracyclines on cellular iron metabolism are essential for determining the precise mechanisms of cytotoxicity in both neoplastic and myocardial cells. This is crucial for the development of improved anticancer treatments with limited cardiotoxicity.

Under physiological conditions, iron is delivered to cells via the binding of transferrin (Tf) to the TfR1 located on the cell membrane. The Tf-TfR1 complex is internalized into the cell

Children's Cancer Institute Australia for Medical Research is affiliated with the University of New South Wales and Sydney Children's Hospital. The work was supported by a Ph.D. scholarship (to J.C.K.) and grant (D.R.R.) from the National Heart Foundation and by a fellowship and grants from the National Health and Medical Research Council (to D.R.R.).

ABBREVIATIONS: TfR1, transferrin receptor 1; DOX, doxorubicin; E64d, (2*S*,3*S*)-*trans*-epoxysuccinyl-L-leucylamido-2-methylbutane ethyl ester; MG132, *N*-benzoyloxycarbonyl (*Z*)-Leu-Leu-leucinal; MEM, minimum essential medium; SMM, stromal-mitochondrial membrane; Tf, transferrin; PAGE, polyacrylamide gel electrophoresis; MnTBAP, Mn(III)tetrakis(4-benzoic acid)-porphyrin.

via receptor-mediated endocytosis (Kwok and Richardson, 2002b). A decrease in endosomal pH releases the iron from Tf. The iron is then transported across the membrane via the divalent metal ion transporter 1 and enters the intracellular labile iron pool (Kwok and Richardson, 2002b). From this latter compartment, iron can be incorporated into heme and non–heme iron-containing proteins or stored in the protein ferritin (Kwok and Richardson, 2002b). Ferritin consists of 24 subunits of two types, namely heavy and light chains. These subunits are symmetrically organized, generating a cavity within the protein for iron storage (Harrison and Arosio, 1996).

We previously demonstrated that after iron uptake into cells, iron is initially incorporated into ferritin, followed by iron mobilization from ferritin and its redistribution to other cellular compartments (Kwok and Richardson, 2003). This supports the theory that ferritin is not merely an iron-storage molecule, but it can act as an intermediate in iron transport (Speyer and Fielding, 1979). Currently, little is understood regarding the physiological mechanisms of ferritin-iron mobilization. In vitro studies demonstrated that biological reductants including reduced flavins (Funk et al., 1985), superoxide (Bolann and Ulvik, 1987), and ascorbate (Bienfait and Van der Briel, 1980), can promote iron release from ferritin. Studies using isolated ferritin showed that substitution of conserved amino acid residues in the 3-fold axes enhances iron release from ferritin (Jin et al., 2001). In addition, structural changes in ferritin may open channels to facilitate iron mobilization (Funk et al., 1985). However, the physiological significance of these experiments on purified ferritin is uncertain. Others have suggested that ferritin-iron release necessitates the degradation of ferritin within lysosomes (Roberts and Bomford, 1988; Radisky and Kaplan, 1998; Persson et al., 2001). Lysosomes are acidic organelles that contain hydrolases for the degradation and turnover of intracellular molecules (Pillay et al., 2002). Indeed, studies using cultured cells have demonstrated lysosomal degradation of ferritin (Hernandez-Yago et al., 1980; Radisky and Kaplan, 1998).

We showed previously in neoplastic and myocardial cells that anthracyclines inhibit iron mobilization from ferritin, resulting in marked accumulation of ferritin-iron (Kwok and Richardson, 2003). This consequently inhibited iron redistribution from ferritin to other vital iron-containing pathways. Interestingly, anthracyclines can localize in lysosomes (Hurwitz et al., 1997) and disrupt lysosomal morphology and enzyme activity (Singal et al., 1985). However, the possibility that lysosomes are cellular targets of anthracyclines, resulting in the inhibition of lysosome-mediated ferritin degradation and the redistribution of iron to vital cellular processes, has not been investigated.

In the present study we showed that inhibition of energy generation or protein synthesis inhibits the ferritin-iron mobilization pathway. Importantly, a range of lysosomal enzyme inhibitors, lysosomotropic agents, and proteasomal inhibitors resulted in marked ferritin-iron accumulation that was comparable with that found using the anthracycline doxorubicin (DOX). These data provide further evidence of a mechanism involving lysosomes in the degradation of ferritin that is required for the release and redistribution of metabolically useful iron. The inhibition of iron redistribution to other compartments may have detrimental effects on vital iron-dependent processes, and it is possible that the lysosomal degradation pathway represents a potential target for anthracycline cytotoxicity.

Materials and Methods

Cell Treatments and Reagents. Chloroquine, cycloheximide, E64d, horse spleen ferritin, lactacystin, leupeptin, methylamine, MG132, pepstatin A, puromycin, rotenone, sodium azide, and sodium cyanide were obtained from Sigma Chemical Co. (St. Louis, MO). DOX was obtained from Pharmacia (Sydney, Australia). The noncytotoxic DOX aglycone, doxorubicinone, was kindly provided by Drs. B. Binaschi and M. Berettoni (Menarini Ricerche S.p.A., Pomerzia, Italy). All other chemicals were of analytical reagent quality.

Cell Culture. Human SK-Mel-28 melanoma cells were obtained from the American Type Culture Collection (Manassas, VA). Briefly, cells were grown in Eagle's modified minimum essential medium (MEM) (Invitrogen, Sydney, Australia) containing 10% fetal calf serum (Invitrogen), 1% nonessential amino acids (Invitrogen), 100 μg/ml streptomycin (Invitrogen), 100 U/ml penicillin (Invitrogen), and 0.28 μg/ml Fungizone (Squibb Pharmaceuticals, Montréal, Canada). Cells were cultured in an incubator (Thermo Forma, Marietta, OH) at 37°C in a humidified atmosphere of 5% CO_2/95% air and subcultured as described previously (Richardson and Baker, 1990). Cellular growth and viability were assessed by phase-contrast microscopy and Trypan blue staining. The SK-Mel-28 cell type was used as the experimental model to study ferritin-iron accumulation because our previous investigation demonstrated that the same effect was observed with cardiomyocytes and a variety of tumor cell lines (Kwok and Richardson, 2003).

Preparation of ^{59}Fe-Transferrin. Human apotransferrin (Sigma) was labeled with ^{59}Fe (PerkinElmer Life and Analytical Sciences, Boston, MA) to produce $^{59}Fe_2$-transferrin (^{59}Fe-Tf), as described previously (Richardson and Baker, 1990). Unbound ^{59}Fe was removed by vacuum dialysis against 0.15 M NaCl with 1.4% $NaHCO_3$, pH 7.4. Fully saturated diferric Tf was used in all experiments.

Determination of Intracellular Iron Distribution Using Native PAGE-^{59}Fe Autoradiography. Native PAGE-^{59}Fe autoradiography was performed using established techniques (Richardson and Milnes, 1997). Briefly, cells were labeled with ^{59}Fe-Tf ([protein] = 0.75 μM) and then lysed using 55 μl of ice-cold 1.5% Triton X-100 containing 2 mM phenylmethylsulfonyl fluoride (Sigma) followed by one freeze-thaw cycle. Samples were vortexed and centrifuged at 14,000 rpm for 45 min at 4°C to separate the stromal-mitochondrial membrane (SMM) fraction from the cytosolic fraction. Under these conditions, SMM contains the disrupted plasma and nuclear membranes, intracellular membranes, and a variety of organelles including mitochondria and lysosomes (Rickwood and Patel, 1995).

The SMM pellets were further disrupted to examine ^{59}Fe distribution in this fraction (Richardson and Milnes, 1997). The pellets were vigorously vortexed in the presence of 40 μl of ice-cold 1.5% Triton X-100 containing freshly prepared 2 mM phenylmethylsulfonyl fluoride and glass powder (Richardson and Milnes, 1997). Samples were then centrifuged at 14,000 rpm for 45 min at 4°C, and the supernatant was collected.

Cytosolic fractions and/or SMM fractions were loaded onto a 5% native PAGE gel to give equal counts of radioactive ^{59}Fe across all samples. Therefore, the autoradiograph compares the relative intracellular distribution of ^{59}Fe within each fraction, rather than the amount of ^{59}Fe/μg protein. Radioactive counts were determined using a γ-scintillation counter (Amersham Biosciences, Uppsala, Sweden). Similar experiments were also performed loading equal amounts of protein (100 μg) across all samples. Protein concentrations were determined using a protein assay (Bio-Rad, Hercules, CA). Experiments loading equal radioactive counts gave results similar to those obtained using equal protein loading. Electrophoresis was performed at 15 mA/gel for 2 to 3 h at 4°C. Gels were subsequently dried at 80°C, and autoradiography was performed. Bands

on X-ray film were quantified by scanning densitometry using a Laser Densitometer and analyzed by Kodak Biomax I Software (Eastman Kodak, Rochester, NY).

[^{3}H]Leucine Incorporation Assay. To assess cellular protein synthesis, [^{3}H]leucine assays were performed. Cells were seeded onto 96-well plates at 15,000 cells/well and incubated overnight. Cells were then incubated with the agents of interest for 24 h at 37°C, followed by incubation with [^{3}H]leucine (0.67 μCi) for 2 h at 37°C (Amersham Biosciences UK, Ltd., Little Chalfont, Buckinghamshire, UK). Cells were harvested using a MicroCell Harvester (Molecular Devices Skatron, Lier, Norway) onto filter mats, and radioactivity was measured on a β scintillation counter (1205 Betaplate liquid scintillation counter; PerkinElmer Wallac, Turku, Finland). Protein synthesis was determined by the incorporation of [^{3}H]leucine into cells using standard techniques (Richardson and Milnes, 1997).

Lysosomal Enzyme Activity Assay. To determine the activity of a range of lysosomal enzymes, cells were incubated with control media or DOX (5 μM) for 24 h at 37°C. The cell pellets were then lysed by freeze-thawing, and protein concentration was determined using the Lowry method. Enzyme activity was assessed using fluorogenic 4-methyl umbelliferyl substrates at 37°C according to standard clinical procedures (Giljaard, 1980) used at the Department of Chemical Pathology, Women's and Children's Hospital (Adelaide, Australia). Results are expressed as nanomoles of substrate cleaved per minute per milligram of protein.

Statistical Analysis. Experimental data were compared using the Student's t test. Results were considered statistically significant when $p < 0.05$.

Results

Cellular ^{59}Fe Uptake and Intracellular ^{59}Fe Distribution into the Cytosol and Stromal Mitochondrial Membrane Fraction in the Presence and Absence of DOX. We showed previously that incubation of tumor cells and primary cardiomyocyte cultures with DOX resulted in a marked accumulation of ferritin-^{59}Fe compared with control cells (Kwok and Richardson, 2003). These experiments were confined to examining the cytosol, and there was no assessment of ^{59}Fe incorporation in the membrane fraction. It is possible that ^{59}Fe accumulating in ferritin in the presence of DOX was derived from the SMM fraction, a hypothesis that was not examined in our previous investigation (Kwok and Richardson, 2003). Therefore, initially in the present study, we examined the effect of DOX on the intracellular distribution of ^{59}Fe in the cytosolic and SMM fractions. This latter fraction contains disrupted plasma and nuclear membranes, intracellular membranes, and a variety of organelles, including mitochondria and lysosomes (Rickwood and Patel, 1995). These experiments were critical in terms of assessing the mechanism(s) involved in the DOX-mediated ferritin-^{59}Fe accumulation. Examination of ^{59}Fe distribution in the SMM was particularly important considering the role of the mitochondrion and lysosome in iron metabolism (Roberts and Bomford, 1988; Link et al., 1996; Radisky and Kaplan, 1998; Persson et al., 2001) and their potential to be affected by anthracyclines (Singal et al., 1985; Link et al., 1996).

In these experiments, SK-Mel-28 melanoma cells were used to assess the effects of DOX (20 μM) compared with control medium on ^{59}Fe uptake from ^{59}Fe-Tf (0.75 μM). Quantitative ^{59}Fe uptake from ^{59}Fe-Tf in control cells was linear as a function of incubation time ($r = 0.99$) (Fig. 1A), as observed in previous studies using this cell type (Richardson and Baker, 1990). Cells incubated with DOX (20 μM) also demonstrated linear ($r = 0.97$) ^{59}Fe uptake from ^{59}Fe-Tf as a function of incubation time (Fig. 1A). Furthermore, DOX (20 μM) had no significant effect on the rate of ^{59}Fe uptake compared with the control (Fig. 1A). Examining the amounts of intracellular ^{59}Fe between the cytosol and SMM fractions, it was evident that most ^{59}Fe was found in the cytosol for

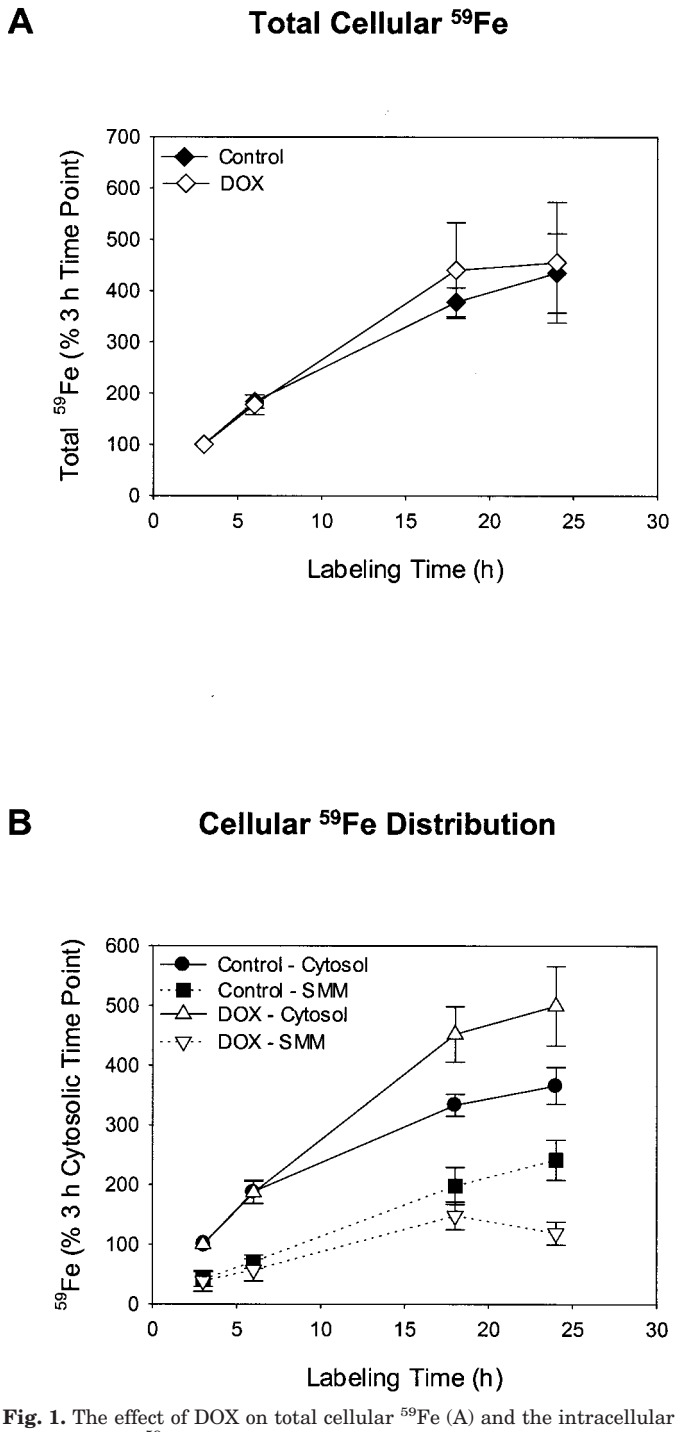

Fig. 1. The effect of DOX on total cellular ^{59}Fe (A) and the intracellular distribution of ^{59}Fe (B) between the cytosol and SMM fractions during incubation of SK-Mel-28 melanoma cells with ^{59}Fe-Tf. The SK-Mel-28 melanoma cells were labeled with ^{59}Fe-Tf (0.75 μM) in the presence or absence of DOX (20 μM) for 3 to 24 h at 37°C and washed, and the intracellular distribution of ^{59}Fe was determined in the cytosol and SMM (as described under *Materials and Methods*). Results shown are mean ± S.D. of three separate experiments performed.

both control and DOX-treated cells (Fig. 1B). After 18 and 24 h, significantly ($p < 0.03$) more ^{59}Fe was detected in the cytosol of DOX-treated cells compared with cells incubated with control medium (Fig. 1B). Conversely, significantly ($p < 0.04$) less ^{59}Fe was found in the SMM fraction in DOX-treated cells compared with control cells, particularly after 24 h (Fig. 1B). These results suggested that for time points beyond 18 h, DOX increased the ratio of ^{59}Fe between the cytosol and SMM during ^{59}Fe uptake from ^{59}Fe-Tf compared with control cells.

The cellular distribution of ^{59}Fe within the cytosol (Fig. 2A) and SMM (Fig. 2C) was then assessed using the native PAGE-^{59}Fe autoradiography technique (Fig. 2, A and C). In these studies, equal amounts of radioactivity were added to each lane of the gel, and the distribution of ^{59}Fe between intracellular molecules was assessed. As described in Fig. 1B, the quantitative amount of ^{59}Fe in the cytosol was greater than that found in the SMM. Considering this, it should be noted that although the ferritin-^{59}Fe bands in Fig. 2, A and C, are of similar intensity, this is because of the different exposure periods used to optimize detection of ^{59}Fe-containing components.

The distribution of cytosolic ^{59}Fe in Figs. 2A and 3A has been reported previously (Kwok and Richardson, 2003), but it was important to include in this study so as to compare the cytosolic and SMM fractions. It was evident that ^{59}Fe distribution was similar in both the cytosol and SMM fractions (Fig. 2, A and C). A large proportion of ^{59}Fe in control and DOX-treated cells was found in a band that comigrated with horse spleen ferritin (Fig. 2, A and C) and could be supershifted with an antiferritin antibody, further confirming its identity (Kwok and Richardson, 2003). Several bands above ferritin and a low molecular mass band were found in both the cytosol and SMM (Fig. 2, A and C). As discussed previously (Kwok and Richardson, 2003), the exact molecular identity of these bands above and below ferritin remain unclear and were not the focus of this investigation.

In both the cytosol and SMM of control cells, ^{59}Fe incorporation in ferritin increased up to 6 h and thereafter decreased to levels observed at the 3-h time point (Fig. 2, A and C, compare lanes 1, 3, 5, and 7; Fig. 2, B and D). In contrast, DOX resulted in marked accumulation of ^{59}Fe in ferritin compared with the control, particularly for incubations of 6 h or more (Fig. 2, A and C, compare lanes 2, 4, 6, and 8; Fig. 2, B and D). Indeed, we have shown previously that after an 18- or 24-h label with ^{59}Fe-Tf in the presence of DOX, ^{59}Fe-ferritin levels were significantly ($p < 0.004$) higher compared with control cells (Kwok and Richardson, 2003). The ^{59}Fe-containing bands above ferritin in the SMM were more pronounced in control cells than in those incubated with DOX after incubations of 18 or 24 h (Fig. 2C; compare lanes 5 and 7 with lanes 6 and 8). This suggested that in contrast to control cells, DOX resulted in the majority of ^{59}Fe being incorporated into ferritin with very little being distributed to other compartments. The presence of ferritin in the SMM is of interest, because although ferritin is a cytosolic protein, there are reports of ferritin associated with lysosomes, where it could be catabolized (Roberts and Bomford, 1988; Radisky and Kaplan, 1998; Persson et al., 2001). Alternatively, recently a mitochondrial ferritin has been discovered that is believed to play a role in iron metabolism (Corsi et al., 2002). Therefore, we cannot discount that at least some of the ^{59}Fe detected in the SMM may be associated with this latter molecule.

Cellular ^{59}Fe Redistribution into the Cytosol and Stromal Mitochondrial Membrane Fraction in the Presence and Absence of DOX. Our previous study demonstrated that DOX inhibits the redistribution of ^{59}Fe from cytosolic ferritin, resulting in a marked accumulation within this molecule (Kwok and Richardson, 2003). We investigated using pulse-chase experiments if the cytosolic ferritin-^{59}Fe accumulation was caused by the redistribution of ^{59}Fe from the SMM to the cytosol. Cells were incubated with ^{59}Fe-Tf (0.75 μM) for 3 h at 37°C, washed, and reincubated in control media or media containing DOX (20 μM) for 0 to 24 h.

Quantitative analysis of ^{59}Fe levels demonstrated that the total ^{59}Fe in both control and DOX-treated cells decreased as a function of reincubation time, with there being no significant difference between the two groups (Fig. 3A). Examination of the cytosol and SMM demonstrated that ^{59}Fe levels in these fractions also decreased as a function of incubation time in both control and DOX-treated cells (Fig. 3B). However, there was no significant difference in ^{59}Fe levels in the cytosol and SMM between control and DOX-treated cells (Fig. 3B). The decrease in cellular ^{59}Fe levels was caused by the efflux of ^{59}Fe into the reincubation medium that occurs in the presence of 10% FCS but not in its absence (data not shown; Richardson and Baker, 1990). The reason for this considerable release of ^{59}Fe in the presence of serum is unclear but could be related to the presence of the ferroxidase ceruloplasmin that acts to mobilize ^{59}Fe from cells (Richardson, 1999).

The distribution of ^{59}Fe within the cytosol and SMM was then assessed after the initial 3-h labeling period with ^{59}Fe-Tf (Fig. 4, A and C). Reincubation of cells in control media for 3 or 6 h markedly increased the incorporation of ^{59}Fe in cytosolic and SMM ferritin (Fig. 4, A and C; compare lane 1 with lanes 2 and 4). However, after a longer chase period of 18 to 24 h in control media, the incorporation of ^{59}Fe in ferritin markedly decreased to levels comparable with that observed at the 0-h time point (Fig. 4, A and C; compare lanes 2 and 4 with lanes 6 and 8; Fig. 4, B and D). Notably, in control cells at the 18- and 24-h time points, ^{59}Fe could be detected in a range of diffuse higher molecular mass bands in the cytosol and SMM (Fig. 4, A and C, lanes 6 and 8). These results indicate that in control cells, ^{59}Fe was initially incorporated into ferritin, but it is later mobilized from this molecule and relocated to other compartments within both the cytosol and SMM. These experiments support our previous study examining cytosolic ^{59}Fe distribution (Kwok and Richardson, 2003).

When DOX was present during the chase period, ^{59}Fe incorporation into ferritin continued to increase with reincubation time, resulting in a marked accumulation of ^{59}Fe-ferritin in the cytosol and SMM (Fig. 4, A and C, lanes 3, 5, 7, and 9; Fig. 4, B and D). Indeed, our earlier studies have demonstrated that after an 18- or 24-h reincubation with DOX, a significant ($p < 0.0003$) accumulation of ^{59}Fe-ferritin was observed compared with control cells (Kwok and Richardson, 2003). In contrast to control cells, there was little evidence of ^{59}Fe localization in other bands above or below the ferritin band in DOX-treated cells (Fig. 4, A and C; compare lanes 6 and 7, lanes 8 and 9).

Effect of an Anthracycline Aglycone on ^{59}Fe Incorporation into Ferritin. We investigated whether the inhibition of iron mobilization from ferritin was a nonspecific cytotoxic response after anthracycline treatment. Because the aminosugar on the anthracycline molecule is believed to be an important structural requirement for the cytotoxic and

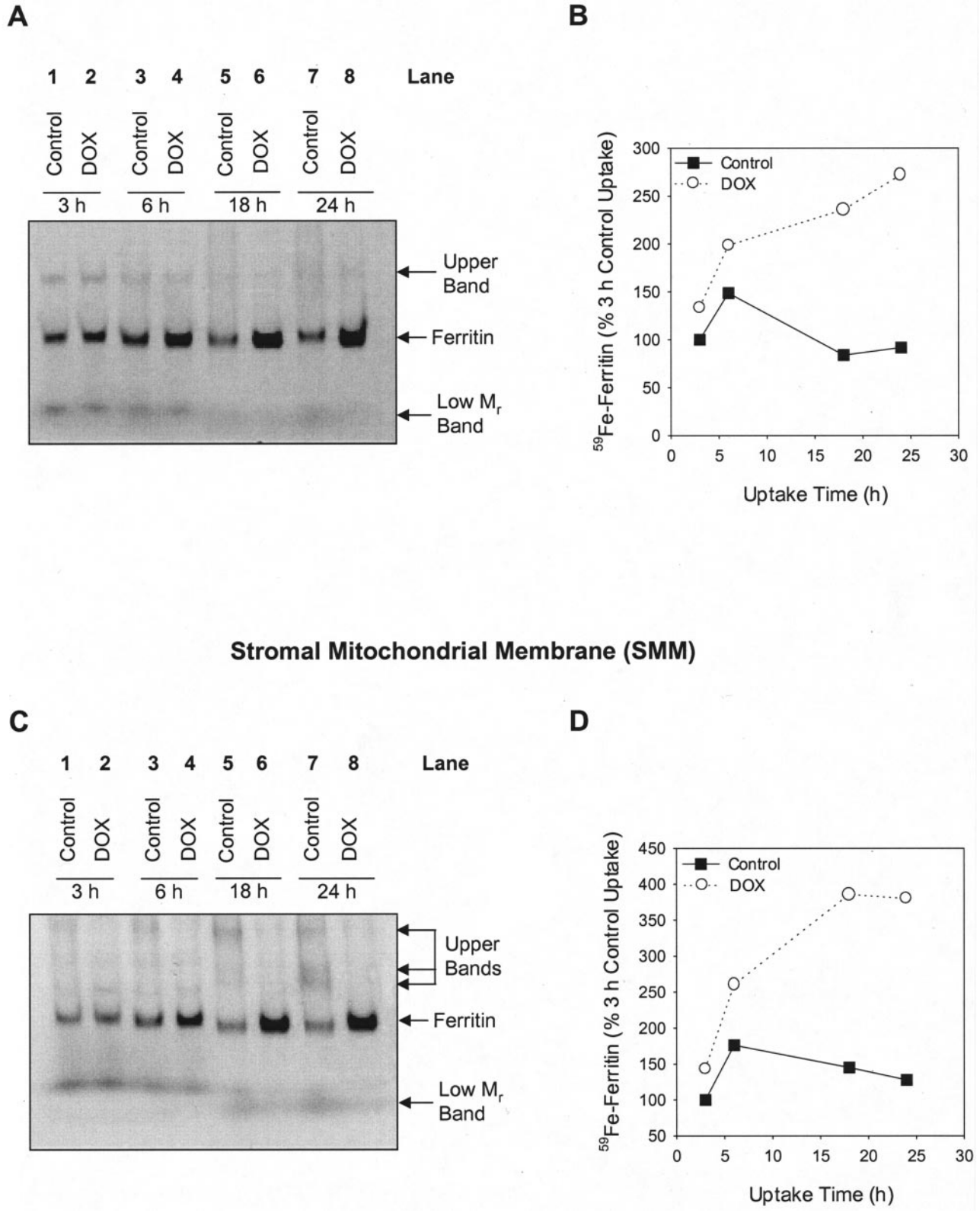

Fig. 2. Doxorubicin results in marked accumulation of ^{59}Fe in cytosolic and SMM ferritin of SK-Mel-28 melanoma cells during ^{59}Fe uptake from ^{59}Fe-Tf. SK-Mel-28 cells were incubated with ^{59}Fe-Tf (0.75 μM) for 3 to 24 h at 37°C in the presence or absence of DOX (20 μM). Native PAGE-^{59}Fe autoradiography was performed on the cytosolic fraction (A) and the SMM fraction (C) as described under *Materials and Methods*. B and D are densitometric analyses of A and C, respectively. Results shown are a typical experiment of three performed.

DNA-binding activity of anthracyclines (Zunino et al., 2001), we examined the less cytotoxic DOX aglycone, doxorubicinone, that lacks the sugar moiety (Zunino et al., 2001). In these experiments, SK-Mel-28 cells were labeled with ^{59}Fe-Tf for 3 h, washed, and reincubated in control media, DOX (5 and 10 μM), or doxorubicinone (5 and 10 μM) for 18 h at 37°C.

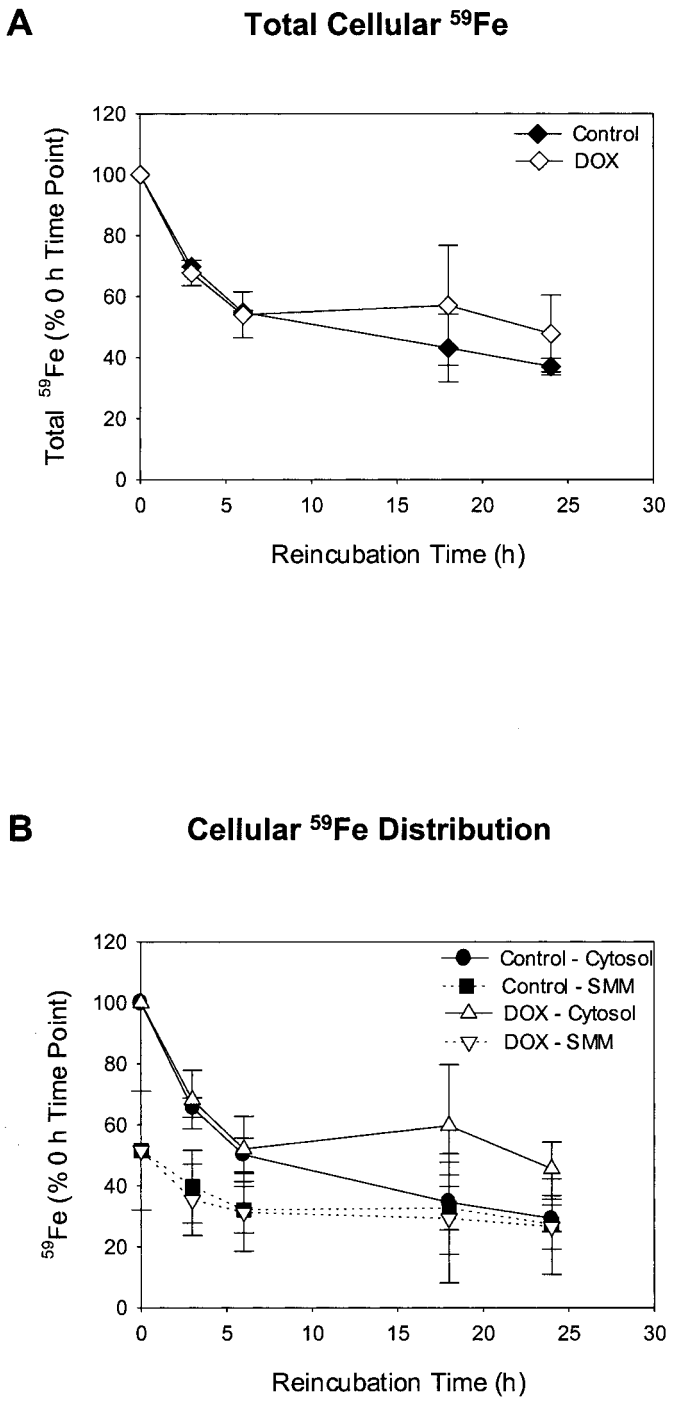

Fig. 3. The effect of a pulse-chase incubation with DOX or control media on total cellular ^{59}Fe (A) and the redistribution of ^{59}Fe (B) between the cytosol and SMM fractions in SK-Mel-28 melanoma cells prelabeled with ^{59}Fe-Tf. The SK-Mel-28 cells were prelabeled with ^{59}Fe-Tf (0.75 μM) for 3 h at 37°C and washed. This was followed by a 0- to 24-h chase period at 37°C in control media or media containing DOX (20 μM). Results shown are mean ± S.D. of three separate experiments performed.

Incubation of cells with the aglycone doxorubicinone (5 and 10 μM) resulted in no cytotoxicity, as demonstrated by the absence of cell death and morphological changes compared with control cells (data not shown). As observed previously, DOX at both 5 and 10 μM resulted in a marked 5- to 7-fold accumulation of ^{59}Fe in ferritin compared with control cells (Fig. 5A; compare lanes 1 and 2, lanes 4 and 5; Fig. 5B). Cells incubated with 5 μM doxorubicinone resulted in a 1.8-fold increase in ^{59}Fe-ferritin levels compared with the control (Fig. 5A; compare lanes 1 and 3; Fig. 5B). Higher concentrations of 10 μM doxorubicinone caused a 3-fold increase in ^{59}Fe-ferritin compared with control cells (Fig. 5A; compare lanes 3 and 6; Fig. 5B). However, the ability of doxorubicinone to accumulate ^{59}Fe in ferritin was less than that observed in DOX-treated cells (Fig. 5A; compare lanes 2 and 3, lanes 5 and 6; Fig. 5B). Hence, even the noncytotoxic aglycone resulted in an accumulation of iron in ferritin, suggesting that the effect of DOX on increasing ferritin iron levels was not caused by its cytotoxic effect. Moreover, the less pronounced effect of the doxorubicin aglycone on inducing ferritin iron accumulation compared with DOX suggests that the aminosugar residue of DOX is an active moiety that contributes to this effect.

Indeed, the ability of DOX to induce ^{59}Fe accumulation in ferritin has been observed even at 1 μM DOX, and this effect plateaued at approximately 5 μM DOX (Kwok and Richardson, 2003). After a 24-h incubation of cells with these lower concentrations of DOX, little cell death was observed (Kwok and Richardson, 2003). In addition, previous experiments with another commonly used cytotoxic agent, cisplatin, had far less effect on ^{59}Fe-ferritin accumulation compared with cells incubated with DOX. This was despite the marked cell death observed with cisplatin-treated cells compared with cells incubated with DOX (Kwok and Richardson, 2003). Hence, the ability of DOX to inhibit ^{59}Fe mobilization from ferritin does not seem to simply be a nonspecific cytotoxic effect.

Collectively, the above studies suggest that the presence of DOX inhibited the normal redistribution of ^{59}Fe from ferritin to other molecules in the cytosol and SMM. Considering the possible role of lysosomes in ferritin-iron release (Roberts and Bomford, 1988; Radisky and Kaplan, 1998; Persson et al., 2001), the accumulation of ferritin-^{59}Fe in the cytosol and SMM of DOX-treated cells, but not control cells, could suggest that DOX was inhibiting lysosomal catabolism of ferritin.

In the experiments described below, we investigated the effects of a variety of well-characterized metabolic inhibitors, protein synthesis inhibitors, lysosomal enzyme inhibitors, proteasome inhibitors, and lysosomotropic agents to further understand the mechanisms involved in the DOX-mediated accumulation of ferritin-^{59}Fe.

Metabolic Inhibitors Induce Ferritin-^{59}Fe Accumulation. We showed that DOX induces ferritin-^{59}Fe accumulation by preventing ^{59}Fe mobilization from cytosolic and SMM ferritin (Fig. 4, A and C) (Kwok and Richardson, 2003). At present, little is known about the mechanisms of iron release from ferritin, although the lysosome has been implicated in this process through its ability to catabolize the molecule (Roberts and Bomford, 1988; Radisky and Kaplan, 1998; Persson et al., 2001). Alternatively, iron mobilization may occur by the reduction of Fe(III) to Fe(II) in the ferritin

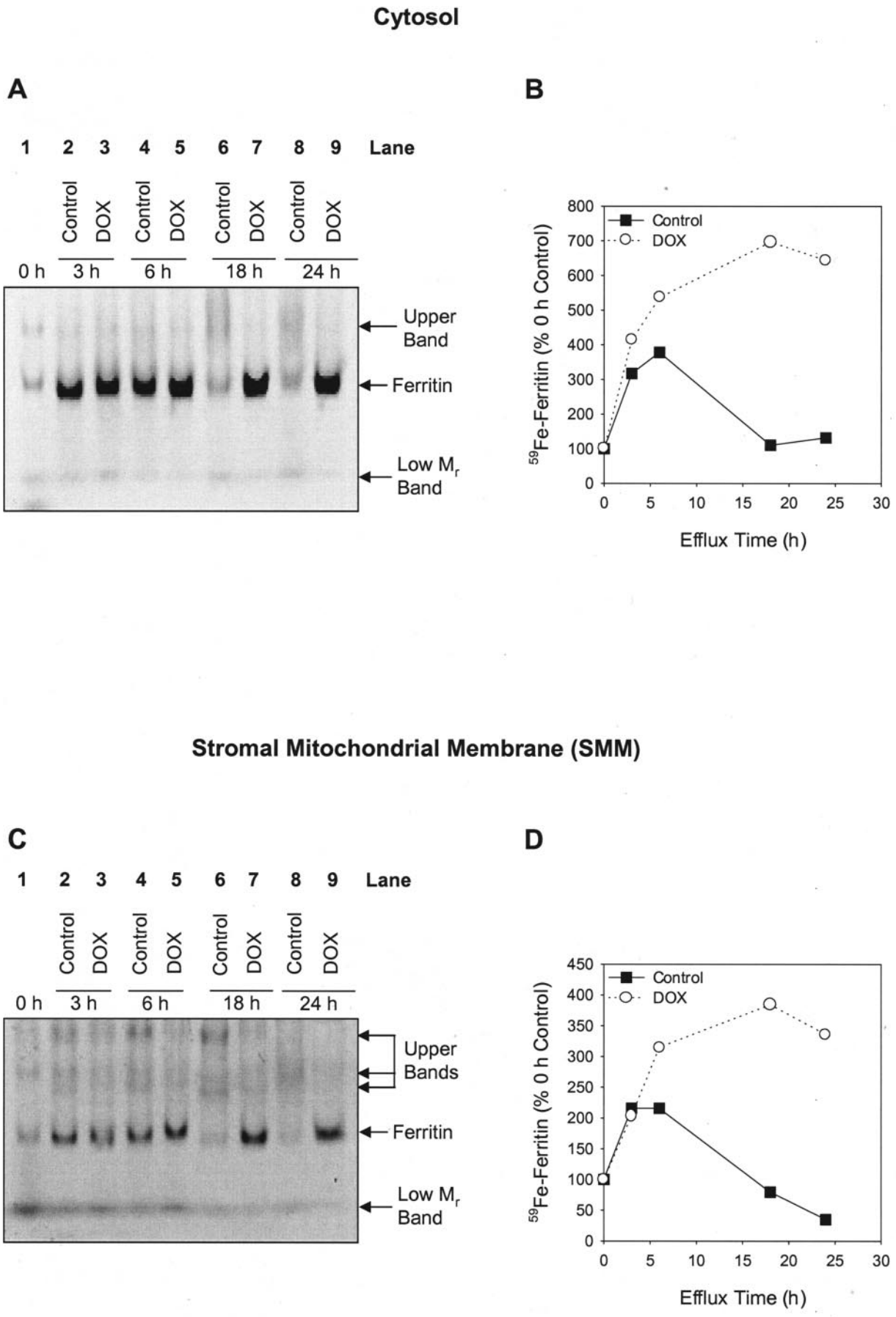

Fig. 4. DOX prevents the redistribution of ^{59}Fe from ferritin in the cytosol and SMM of SK-Mel-28 melanoma cells. Cells were prelabeled with ^{59}Fe-Tf (0.75 μM) for 3 h at 37°C and then washed. This was then followed by reincubation in control media or media containing DOX (20 μM) for 0 to 24 h at 37°C. The cytosolic (A) and SMM (C) fractions were separated, and native PAGE-^{59}Fe autoradiography was performed on each fraction (see *Materials and Methods*). B and D are densitometric analyses of A and C, respectively. The results are a typical experiment from three performed.

core by an unknown reductase or reducing factor (Harrison and Arosio, 1996). Irrespective of the mechanism(s) involved, metabolic energy will probably be essential for the process. Considering this, the effect of three well-known metabolic inhibitors on the accumulation of ^{59}Fe in ferritin were examined (Fig. 6, A and B).

Pulse-chase experiments were performed by prelabeling cells with ^{59}Fe-Tf for 6 h, followed by washing and reincubation of cells for 18 h with control media, DOX (10 or 20 μM), NaN_3 (5 or 30 mM), NaCN (1 or 5 mM), or rotenone (10 or 50 μM). We have shown previously that these concentrations effectively decrease cellular ATP levels (Watts and Richardson, 2001; Kwok and Richardson, 2003). As found for DOX, all metabolic inhibitors induced ferritin-^{59}Fe accumulation compared with the control (Fig. 6, A and B). Unexpectedly, cyanide at the higher concentration of 5 mM was less effective than at 1 mM in terms of inducing ferritin-^{59}Fe accumulation. The reason for this is uncertain at present, but it is possible that 5 mM cyanide caused cytotoxicity before any changes in ^{59}Fe-ferritin levels occurred in the cell. Collectively, the results indicate that ferritin-^{59}Fe mobilization is an energy-dependent event.

Inhibition of Protein Synthesis by Cycloheximide Inhibits Iron Mobilization and Results in the Accumulation of ^{59}Fe in Ferritin. Anthracyclines are known to depress cellular protein synthesis (Gianni and Myers, 1992), and it is possible that this latter activity could prevent ferritin-^{59}Fe mobilization and induce iron accumulation in this molecule. Because lysosomes may be involved in ferritin-iron mobilization (Hernandez-Yago et al., 1980; Radisky and Kaplan, 1998) and because lysosomal function requires the continuous synthesis of lysosomal enzymes and proteins (Pillay et al., 2002), it was important to assess the effects of inhibiting protein synthesis on ferritin-^{59}Fe accumulation. In the experiments below, we investigated the effect of the well-known protein synthesis inhibitor cycloheximide on ferritin-^{59}Fe accumulation (Fig. 7).

Pulse-chase experiments were performed by incubating cells with ^{59}Fe-Tf (0.75 μM) for 6 h at 37°C, followed by washing and reincubation with control media, cycloheximide (20–140 μM), or DOX (5 μM) for 18 h at 37°C (Fig. 7, A and B). These concentrations were in the effective range used in the literature (Darnell and Richardson, 1999). Cycloheximide at all concentrations (20–140 μM) resulted in a marked 9- to 10-fold increase in ^{59}Fe-ferritin levels compared with cells incubated with control media alone (Fig. 7, A and B; compare lane 1 with lanes 2–4). This accumulation was comparable with the 8-fold accumulation of ^{59}Fe-ferritin caused by 5 μM DOX (Fig. 7, A and B; compare lanes 1 and 5). Another protein synthesis inhibitor, puromycin (5–200 μM), was also

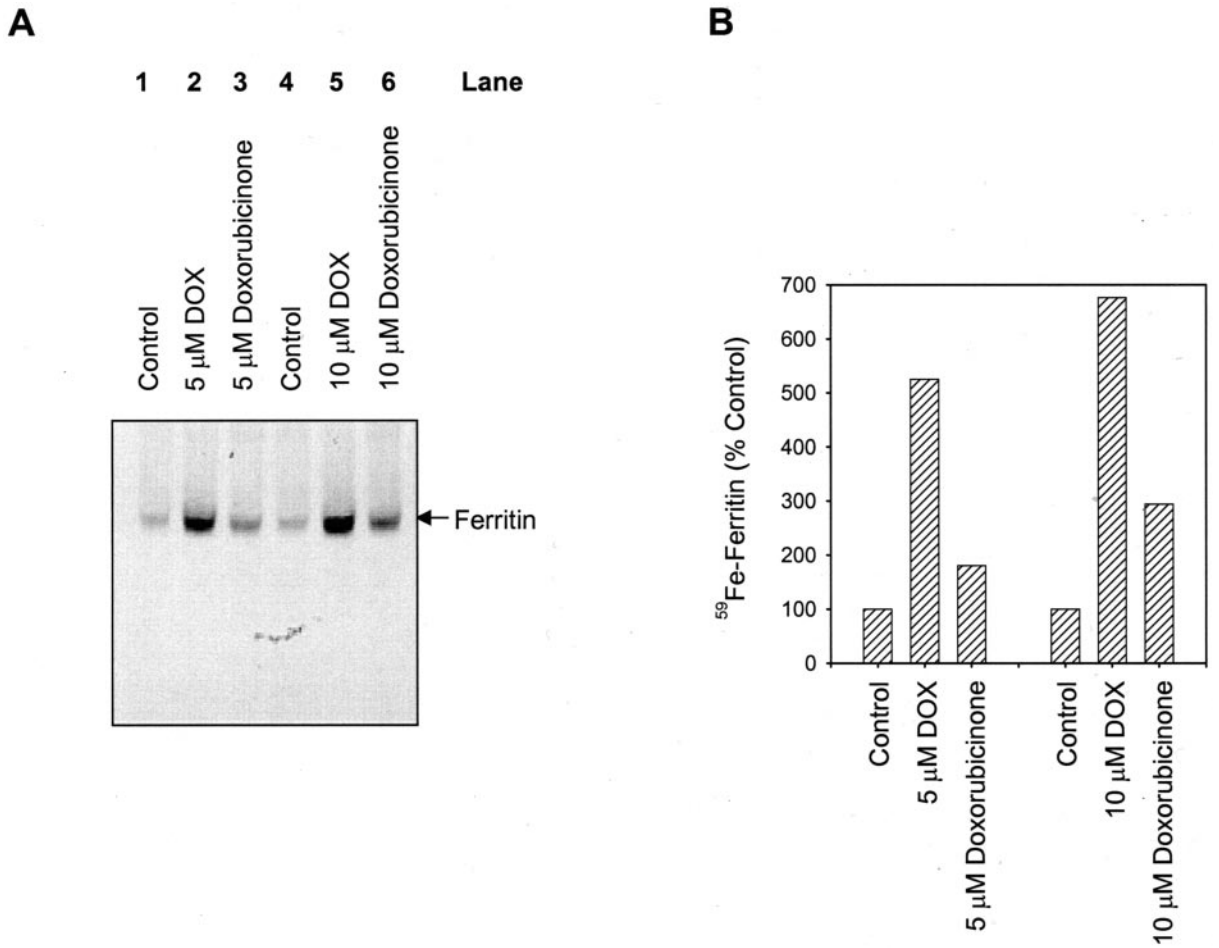

Fig. 5. The anthracycline aglycone doxorubicinone results in ^{59}Fe-ferritin accumulation, but to a much lesser extent than DOX. SK-Mel-28 cells were prelabeled with ^{59}Fe-Tf (0.75 μM) for 3 h at 37°C, washed, and reincubated in control media, DOX (5 and 10 μM), or doxorubicinone (5 and 10 μM) for 18 h at 37°C. Native PAGE-^{59}Fe autoradiography (A) and densitometric analyses (B) were performed. Results are a typical experiment from two performed.

assessed, and like cycloheximide, it prevented ^{59}Fe mobilization and resulted in marked ferritin-^{59}Fe accumulation (data not shown). These studies showed that, similar to DOX, the inhibition of cellular protein synthesis by cycloheximide or puromycin could prevent ferritin-^{59}Fe mobilization.

To further confirm the role of protein synthesis in the redistribution of ^{59}Fe-ferritin, cells exposed to cycloheximide were allowed to recover by washing and reincubation in medium alone. In these studies, cells were labeled with ^{59}Fe-Tf for 6 h at 37°C, washed, and reincubated in cycloheximide (20 μM) for 18 h at 37°C. Cells were then washed again and reincubated for 0 to 24 h in media (MEM) alone before^{59}Fe-PAGE autoradiography (Fig. 7, C and D). The ^{59}Fe-ferritin levels after a 3-h reincubation in cycloheximide-free media decreased slightly compared with cells not reincubated in media (Fig. 7C, compare lanes 1 and 2; Fig. 7D). However, after a 6-h reincubation in cycloheximide-free media, ^{59}Fe-ferritin levels decreased to 43% compared with the 0-h time point (Fig. 7, C, compare lanes 1 and 3, and D). After a 24-h reincubation in cycloheximide-free medium, 93% of ^{59}Fe had been mobilized from ferritin (Fig. 7, C, compare lanes 1 and 5, and D). These results demonstrate that after the removal of cycloheximide, cells were able to recover their ability to mobilize ^{59}Fe from ferritin.

Inability of Cells to Recover ^{59}Fe Mobilization from Ferritin after DOX Treatment. The above studies demonstrated that cycloheximide acts similarly to DOX to induce ferritin-^{59}Fe accumulation, and this was at least partially reversible when the inhibitor was removed (Fig. 7, C and D). Experiments were then performed to determine whether ferritin-^{59}Fe accumulation after exposure to DOX could be reduced upon reincubation with DOX-free media (i.e., MEM). Cells were prelabeled with ^{59}Fe-Tf, washed, and reincubated with control media, DOX (1–5 μM), or cycloheximide (20 μM) for 18 h at 37°C. In parallel samples, cells were washed and then further reincubated for 24 h in media to allow recovery from DOX or cycloheximide (Fig. 8).

Low concentrations of DOX (1–2 μM) only slightly increased ^{59}Fe-ferritin levels compared with control cells (Fig. 8, A and B; compare lane 1 with lanes 2 and 3). However, DOX (5 μM), and to a greater extent cycloheximide (20 μM), markedly increased ^{59}Fe-ferritin levels compared with the control (Fig. 8, A and B, compare lane 1 with lanes 4 and 5). Despite a further 24-h reincubation with DOX-free media, ^{59}Fe-ferritin accumulation in DOX-treated cells decreased only slightly or remained unchanged compared with cells not reincubated in MEM (Fig. 8, A and B; compare lanes 2–4 with lanes 7–9). However, as seen previously (Fig. 7, C and D), reincubation of cycloheximide-treated cells in MEM markedly decreased ^{59}Fe accumulation in ferritin (Fig. 8, A and B; compare lanes 5 and 10). These results suggested that the mechanism by which DOX inhibits ^{59}Fe mobilization from

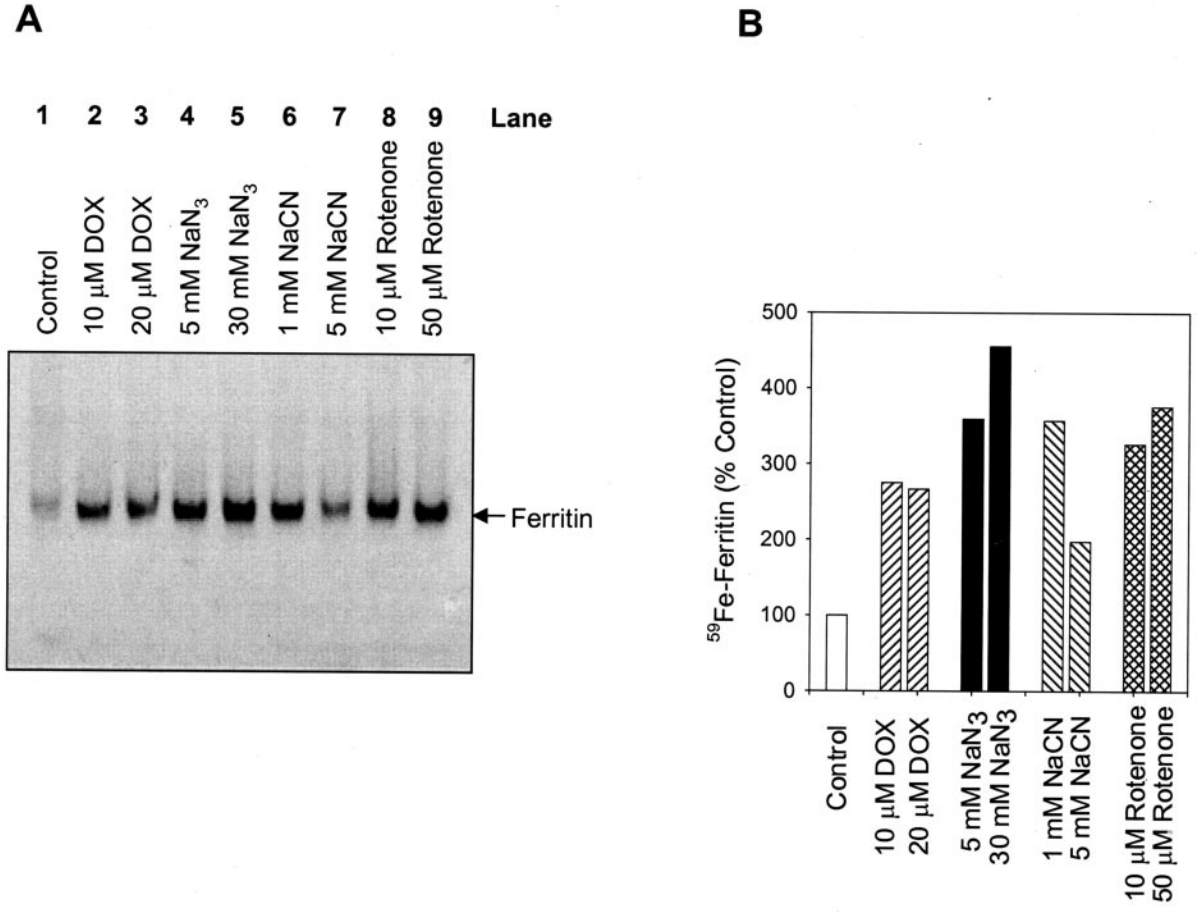

Fig. 6. Metabolic inhibitors prevent ^{59}Fe mobilization from ferritin in SK-Mel-28 melanoma cells. The cells were prelabeled with ^{59}Fe-Tf (0.75 μM) for 6 h at 37°C, washed, and then reincubated for 18 h at 37°C with control media, DOX (10 and 20 μM), or the metabolic inhibitors NaN_3 (5 or 30 mM), NaCN (1 or 5 mM), or rotenone (10 or 50 μM). Cellular ^{59}Fe distribution was assessed using native PAGE-^{59}Fe autoradiography (A) (see *Materials and Methods*) and densitometric analysis (B) of A. Results shown are a typical experiment from two performed.

ferritin was not reversible despite removal of the agent from the incubation media. It is likely that DOX remains trapped within the cell even upon reincubation in DOX-free media.

Recovery of Protein Synthesis Upon Removal of Cycloheximide or Doxorubicin. We demonstrated above that incubation of SK-Mel-28 melanoma cells with cycloheximide or DOX resulted in marked ferritin-^{59}Fe accumulation (Figs. 7 and 8). This inhibition could be relieved when cycloheximide was removed from the cells, resulting in mobilization of ^{59}Fe from ferritin (Figs. 7 and 8). However, ferritin-

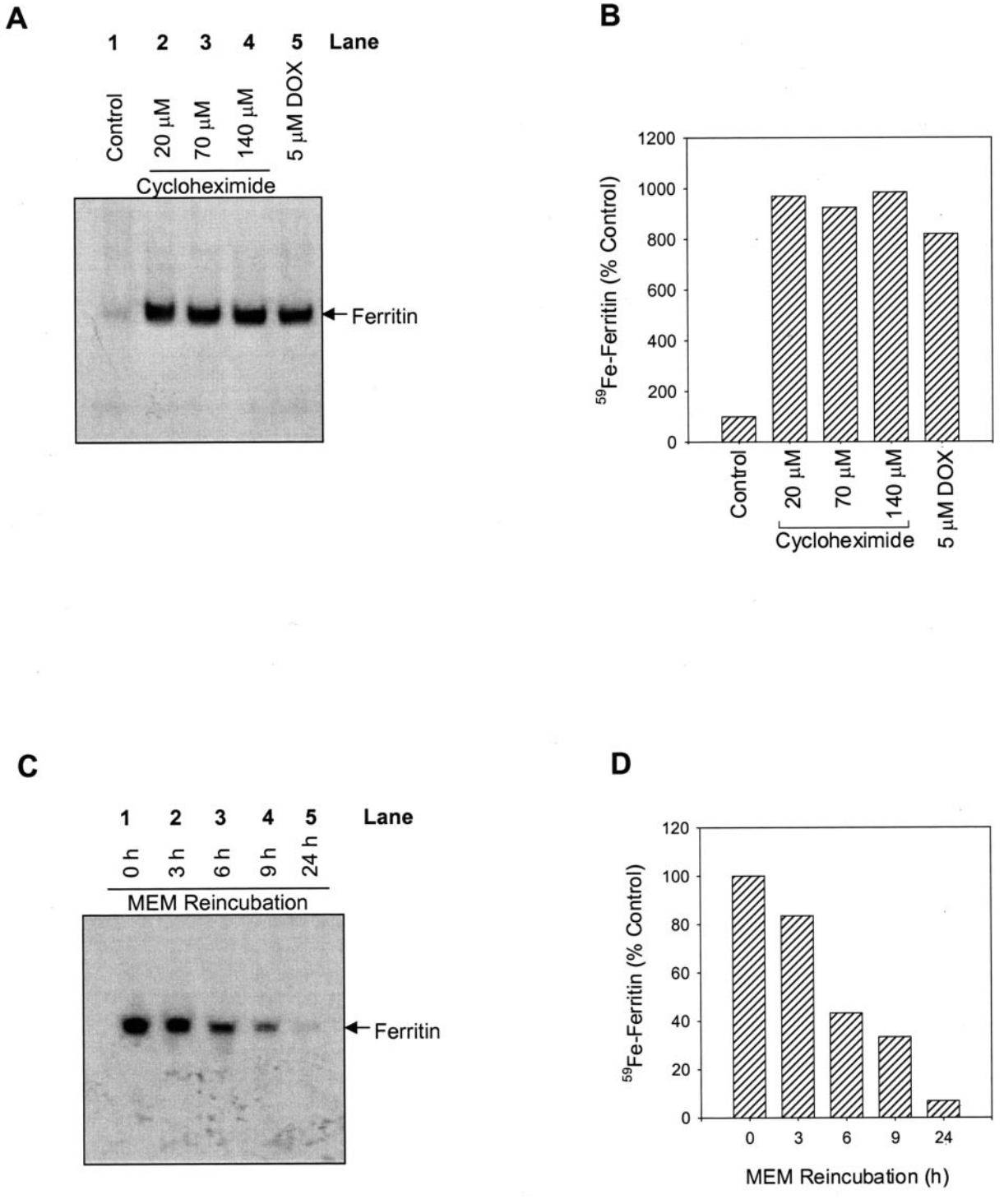

Fig. 7. Inhibition of cellular protein synthesis by cycloheximide results in accumulation of ^{59}Fe in ferritin in SK-Mel-28 melanoma cells, and this is reversible upon removal of cycloheximide. A, the cells were prelabeled for 6 h at 37°C with ^{59}Fe-Tf (0.75 μM) and washed. The cells were then reincubated with control media, cycloheximide (20–140 μM) or DOX (5 μM) for 18 h at 37°C, and native PAGE-^{59}Fe autoradiography was performed (see *Materials and Methods*). B, densitometric analysis of A. C, cells were prelabeled with ^{59}Fe-Tf (0.75 μM) for 6 h at 37°C, washed, and then incubated for 18 h at 37°C with media containing cycloheximide (20 μM). This was followed by washing and a 0- to 24-h reincubation in cycloheximide-free media (MEM) before native PAGE-^{59}Fe autoradiography. D, densitometric analysis of C. Results shown are a typical experiment from three performed.

^{59}Fe accumulation observed after incubation with DOX could not be reversed by reincubation with DOX-free media (Fig. 8). To determine whether these results correlated to the recovery of protein synthesis after removal of the test agents, [^{3}H]leucine assays were performed (Fig. 9).

Cells were incubated with control media, cycloheximide (0.14–18 μM) or DOX (0.02–20 μM) for 18 h, and total [^{3}H]leucine incorporation was assessed. In a parallel set of experiments, cells incubated with these concentrations of cycloheximide or DOX were washed and then reincubated for 24 h at 37°C with media alone (MEM) before assessing [^{3}H]leucine incorporation (Fig. 9).

Figure 9 shows that cycloheximide and DOX were extremely effective at inhibiting cellular protein synthesis in a concentration-dependent manner (Fig. 9, A and B). Interestingly, when cycloheximide-treated cells were reincubated

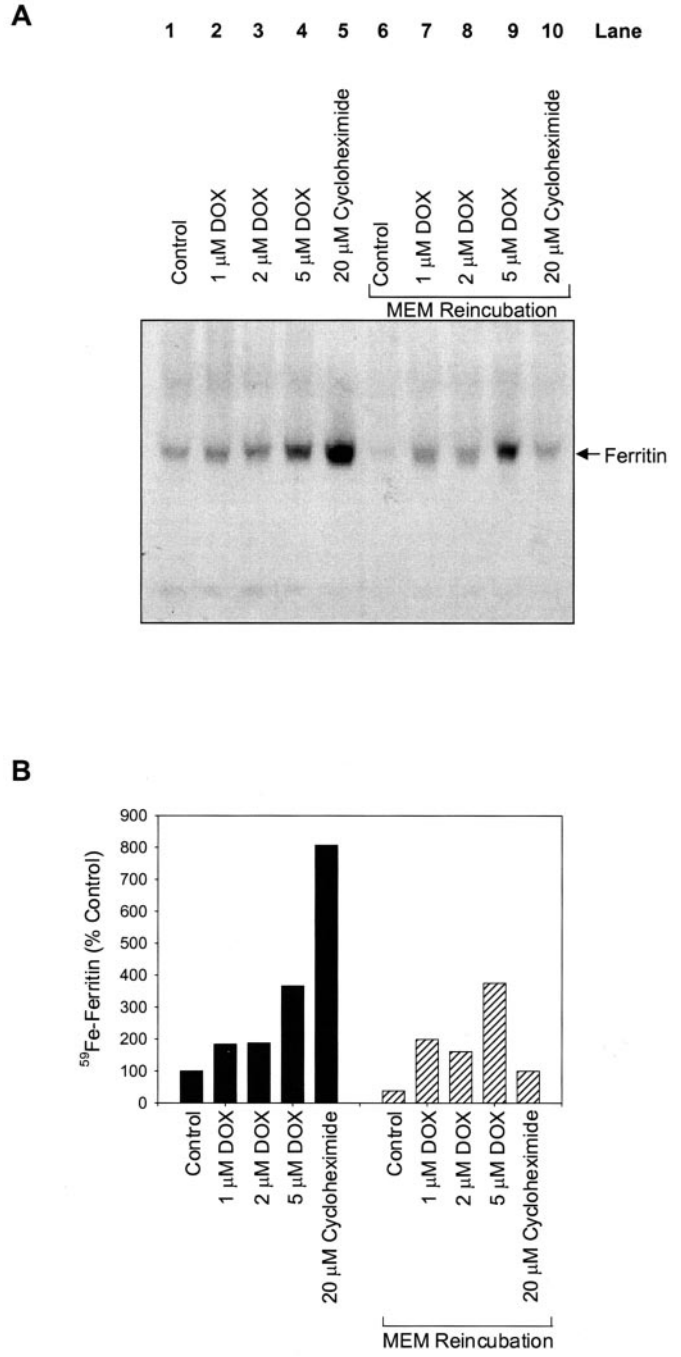

Fig. 8. The accumulation of ^{59}Fe in ferritin observed after incubation with DOX was irreversible despite removal of the drug. A, the SK-Mel-28 cells were prelabeled with ^{59}Fe-Tf (0.75 μM) for 6 h at 37°C, washed, and then reincubated for 18 h at 37°C with control media, DOX (1–5 μM), or cycloheximide (20 μM). In parallel samples, cells were washed and then further reincubated with media alone (MEM) for 24 h at 37°C before native PAGE-^{59}Fe autoradiography. B, densitometric analyses of A. Results are a representative experiment from four performed.

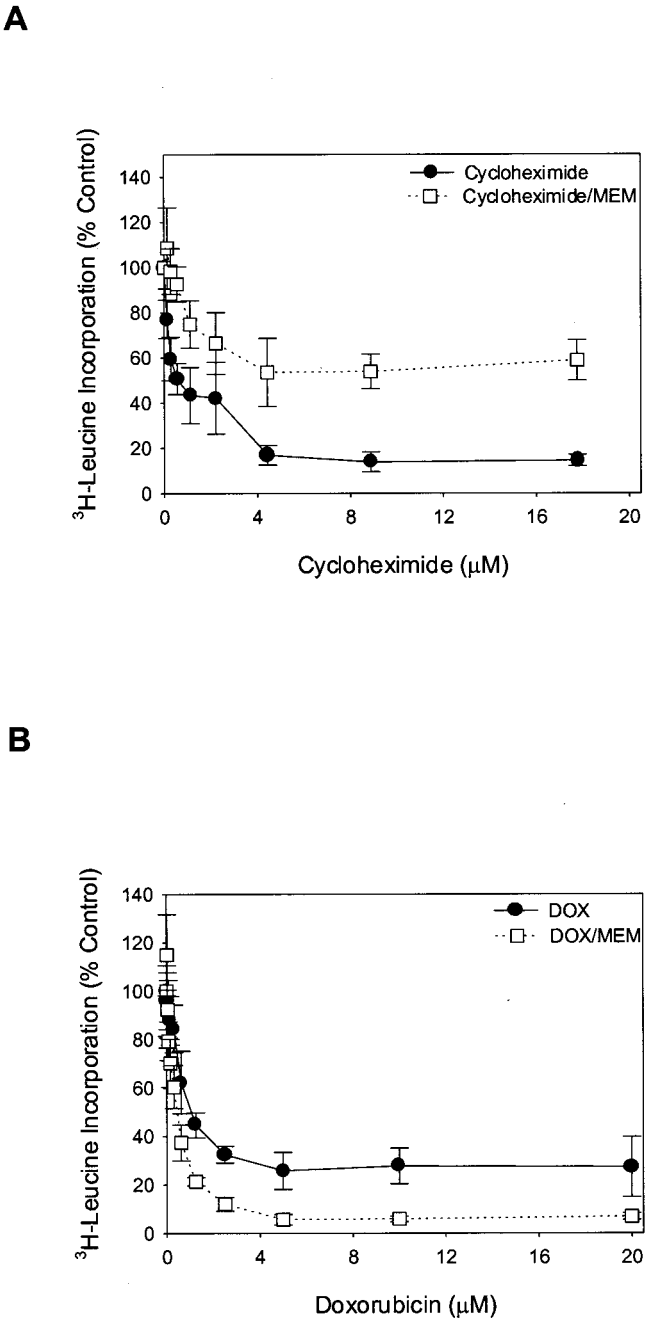

Fig. 9. Protein synthesis in SK-Mel-28 melanoma cells can be partially recovered after removal of cycloheximide, but this does not occur after removal of DOX. The SK-Mel-28 cells were incubated with control media, cycloheximide (0.14–18 μM), or DOX (0.02–20 μM) for 18 h at 37°C, and [^{3}H]leucine incorporation was measured (see *Materials and Methods*). In parallel experiments, cells incubated with these concentrations of cycloheximide or DOX were washed and then reincubated for 24 h at 37°C with media alone (MEM), and [^{3}H]leucine incorporation was assessed. Results are mean ± S.D. from six separate experiments.

with MEM for 24 h, a significant ($p < 0.003$) recovery of protein synthesis was observed at concentrations greater than 4 μM (Fig. 9A). Hence, the recovery of protein synthesis (Fig. 9A) and ^{59}Fe mobilization from ferritin (Fig. 7, C and D) were correlated after the removal of cycloheximide. Despite reincubation in MEM, [^{3}H]leucine incorporation in DOX-treated cells continued to decrease (Fig. 9B). This was significant even in cells previously incubated with only 1 μM DOX ($p < 0.00004$). The inability of cells to recover protein synthesis after treatment with DOX could explain the absence of ^{59}Fe mobilization from ferritin upon removal of DOX from cells (Fig. 8, A and B). Again, this suggests that DOX is still present within the cell despite removal of the agent from the reincubation media. Hence, these studies suggested that mobilization of ^{59}Fe accumulated in ferritin required the recovery of cellular protein synthesis. Furthermore, these results demonstrated that anthracyclines irreversibly inhibit protein synthesis and ^{59}Fe mobilization from ferritin.

Inhibition of Lysosomal Enzymes Inhibits Ferritin-^{59}Fe Mobilization. Previous studies have suggested that the lysosome plays a role in the release of iron from ferritin (Roberts and Bomford, 1988; Radisky and Kaplan, 1998; Persson et al., 2001). Hence, the decrease in ^{59}Fe-ferritin levels and its redistribution to other cellular compartments observed in control cells (Fig. 4, A and C) may be mediated by lysosomal degradation of ferritin (Roberts and Bomford, 1988; Radisky and Kaplan, 1998; Persson et al., 2001). It is also possible that the accumulation of ferritin-^{59}Fe observed in DOX-treated cells (Fig. 4, A and C) was caused by DOX-induced inhibition of lysosomal ferritin degradation. In fact, anthracyclines localize in lysosomes (Hurwitz et al., 1997) and disrupt their morphology and enzyme activity (Singal et al., 1985). Considering this, we assessed the effect of lysosomal enzyme inhibitors on the redistribution of ^{59}Fe from ferritin. Lysosomal enzymes are largely composed of cysteine, aspartic, and serine proteases (Pillay et al., 2002). Hence, we examined the following: pepstatin A, an aspartic protease inhibitor with high specificity for cathepsin D (Knight and Barrett, 1976); E64d, a cysteine protease inhibitor with high specificity for cathepsin B (McGowan et al., 1989); and leupeptin, a general cysteine and serine protease inhibitor (Pillay et al., 2002). In addition, because proteasome-mediated degradation of oxidized ferritin has been reported (Rudeck et al., 2000), we examined the well-characterized proteosome inhibitors MG132 and lactacystin (Lee and Goldberg, 1998).

In these studies, pulse-chase experiments were performed in which cells were labeled with ^{59}Fe-Tf for 6 h at 37°C, washed, and then reincubated for 18 h at 37°C with control media, pepstatin A (100 μM), E64d (100 μM), leupeptin (50 and 100 μM), MG132 (10 μM), lactacystin (10 and 25 μM), or DOX (5 μM). These concentrations were within the effective range used in the literature (Ohshita et al., 1992). Pepstatin A alone had little effect on cytosolic ^{59}Fe-ferritin levels compared with control cells (Fig. 10, A and B, compare lanes 1 and 2), suggesting that aspartic proteases were not involved in ferritin-^{59}Fe mobilization. In contrast, all other lysosomal or proteasomal inhibitors induced ^{59}Fe-ferritin accumulation by 3- to 5-fold compared with control cells (Fig. 10, A and B, compare lane 1 with lanes 3–8). Combination of pepstatin A and E64d gave the same result as treatment with E64d alone (data not shown). Considering these results, the ferritin-^{59}Fe accumulation observed after incubation with DOX could be caused by the inhibition of the lysosome-mediated ferritin degradation pathway.

Inhibition of Lysosomal Acidification Inhibits Ferritin-^{59}Fe Mobilization. To further test the hypothesis that ^{59}Fe release from ferritin involved lysosomes, experiments were performed to inhibit lysosomal acidification that is required for optimal enzymatic activity (Pillay et al., 2002). Pulse-chase experiments were therefore performed using three well-known lysosomotropic agents (NH_4Cl, chloroquine, and methylamine) that increase intralysosomal pH (Ohkuma and Poole, 1978).

In these studies, cells were prelabeled with ^{59}Fe-Tf for 6 h at 37°C, washed, and reincubated with NH_4Cl (1.5 or 15 mM), chloroquine (25 or 250 μM), methylamine (1.5 or 15 mM), or DOX (5 μM) for 18 h at 37°C to assess the role of lysosomal activity in ferritin-^{59}Fe accumulation (Fig. 10, C and D). The lower concentration of each lysosomotropic agent had little effect on ^{59}Fe-ferritin levels compared with control cells (Fig. 10, C, compare lane 1 with lanes 2, 4, and 6, and D). However, at the higher concentrations, NH_4Cl (15 mM), chloroquine (250 μM), and methylamine (15 mM) markedly increased ^{59}Fe-ferritin levels to 3- to 4-fold of that of the control (Fig. 10, C, compare lane 1 with lanes 3, 5, and 7, and D), whereas DOX increased it to 5.5-fold of that of the control value (Fig. 10C, compare lanes 1 and 9). These results with lysosomotropic agents suggest that inhibition of intralysosomal acidification could prevent the mobilization of ferritin-^{59}Fe. These data support our experiments using lysosomal enzyme inhibitors (Fig. 10, A and B). It is of interest to note that the ^{59}Fe-ferritin band observed in cells treated with high concentrations of NH_4Cl, chloroquine, or methylamine was not a well-defined band as seen in control cells (Fig. 10C, compare lane 1 with lanes 3, 5, and 7). The reason for this observation remains unclear at present.

Effect of DOX on Lysosomal Enzyme Activity. Because DOX markedly inhibits cellular protein synthesis (Fig. 9B) (Gianni and Myers, 1992) and inhibition of lysosomal enzyme activity results in marked iron accumulation in ferritin (Fig. 10), it was possible to speculate that this drug targets lysosomal enzyme synthesis, resulting in the inhibition of ferritin degradation and the release of iron from the protein. Hence, the activities of eight lysosomal enzymes were assessed in cells after 24-h incubations with control media or DOX (5 μM). The enzymes examined were the following: β-galactosidase, β-glucuronidase, α-fucosidase, α-mannosidase, β-hexosaminidase A, α-*N*-acetyl-galactosaminidase, arylsulfatase A, and acid phosphatase.

A slight increase in β-galactosidase activity was detected in DOX-treated cells (24 $\pm$ 1 nmol/min/mg protein) compared with control cells (20 $\pm$ 0.1 nmol/min/mg protein), as previously shown by others (Singal et al., 1985). However, DOX did not markedly affect the activity of the other lysosomal enzymes examined (data not shown). These results suggested that inhibition of these lysosomal enzymes was not the primary target of DOX that induces ferritin-^{59}Fe accumulation. However, we cannot discount that other lysosomal enzymes or molecules may be the targets of anthracyclines.

Discussion

We demonstrated previously that anthracyclines inhibit iron mobilization from ferritin in neoplastic cells and cardi-

omyocytes, resulting in a marked accumulation of iron in this molecule (Kwok and Richardson, 2003). We hypothesized that this may represent a potential mechanism of anthracycline cytotoxicity, because the lack of iron redistribution to vital cellular functions may have detrimental effects on the cell (Kwok and Richardson, 2003).

Currently, the mechanisms by which iron is released from ferritin for metabolic use are little understood, but it has been suggested to involve a lysosomal-mediated protein degradation pathway (Roberts and Bomford, 1988; Radisky and Kaplan, 1998; Persson et al., 2001). In the present study, we demonstrated for the first time that ferritin-^{59}Fe mobilization is dependent on metabolic energy and protein synthesis. Moreover, a variety of well-characterized lysosomal enzyme

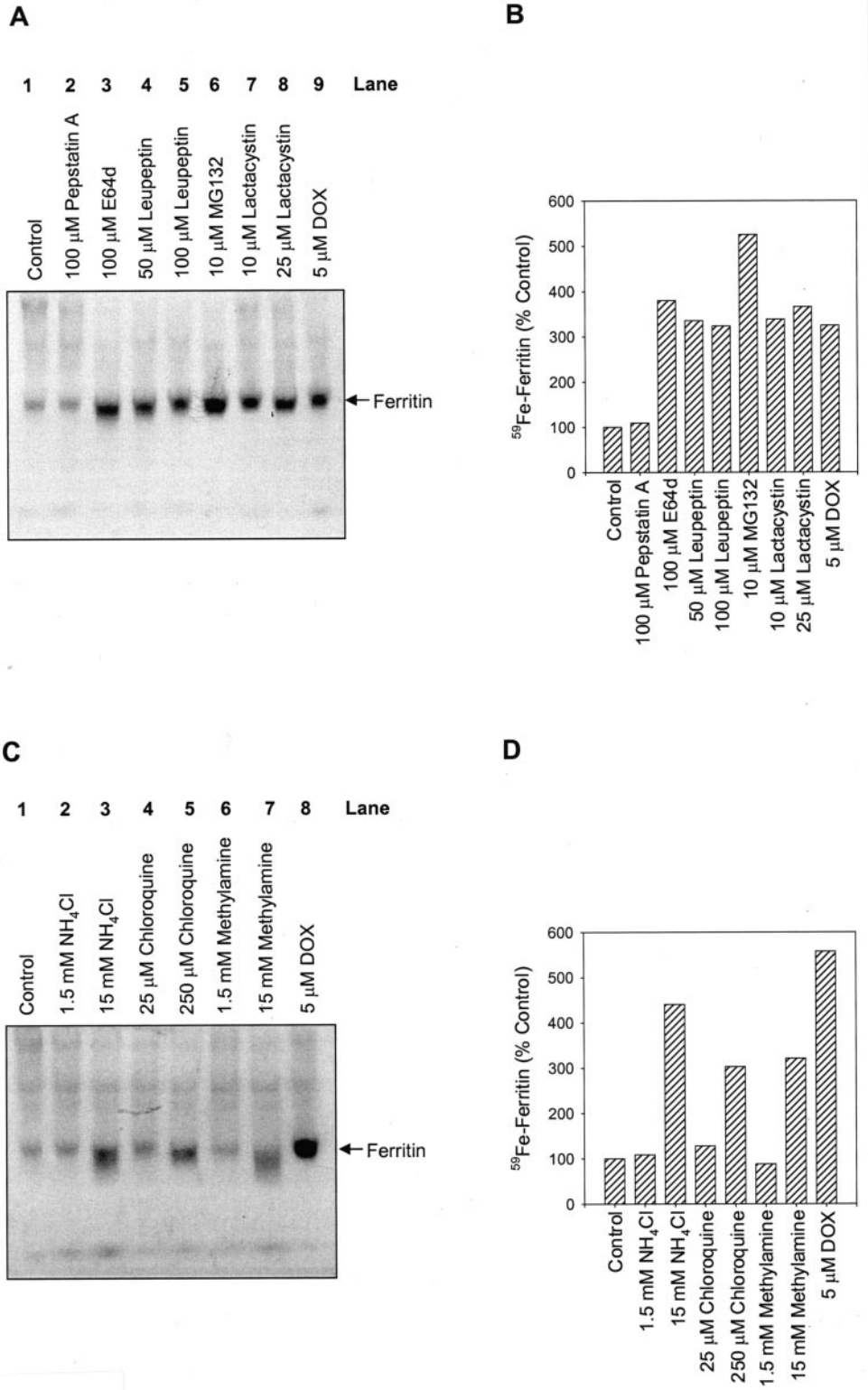

Fig. 10. Inhibition of lysosomal or proteasomal activity results in marked accumulation of ^{59}Fe-ferritin to an extent similar to that found for DOX. A, the SK-Mel-28 cells were labeled with ^{59}Fe-Tf (0.75 μM) for 6 h at 37°C and washed. Cells were then reincubated for 18 h at 37°C in control media, pepstatin A (100 μM), E64d (100 μM), leupeptin (50 or 100 μM), MG132 (10 μM), lactacystin (10 or 25 μM), or DOX (5 μM). Native PAGE-^{59}Fe autoradiography was then performed. B, densitometric analysis of A. C, the SK-Mel-28 melanoma cells were labeled with ^{59}Fe-Tf (0.75 μM) for 6 h at 37°C, washed, and then reincubated with NH_4Cl (1.5 or 15 mM), chloroquine (25 or 250 μM), methylamine (1.5 or 15 mM) or DOX (5 μM) for 18 h at 37°C. Native PAGE-^{59}Fe autoradiography was then performed (see *Materials and Methods*). D, densitometric analysis of C. Results are representative of three or four experiments in A and C, respectively.

inhibitors, lysosomotropic agents, and proteasomal inhibitors resulted in marked accumulation of ferritin-^{59}Fe that was comparable with that found using DOX. These data provide further evidence that DOX inhibits the activity of lysosomes in the degradation of ferritin that is essential for the release and redistribution of metabolically useful iron.

It could be suggested that the effect of DOX on inducing ferritin-^{59}Fe accumulation is a nonspecific cytotoxic response. However, we have shown that the noncytotoxic doxorubicin aglycone doxorubicinone also resulted in accumulation of ^{59}Fe in ferritin (Fig. 5, A and B). In addition, as demonstrated in our previous study (Kwok and Richardson 2003), another commonly used antitumor agent, cisplatin, at 10 μM had little effect on ^{59}Fe accumulation in ferritin compared with control cells, despite being very cytotoxic. Furthermore, as shown in this latter study, low concentrations of DOX (1–5 μM) resulted in marked ferritin iron accumulation, although there was little cell death. Collectively, these results demonstrate that the effect of DOX on inducing ferritin-iron accumulation was not caused by nonspecific cytotoxicity.

The lysosome plays a major role in the normal degradation and recycling of cellular proteins for anabolic use. To date, no study has examined the effect of anthracyclines on ferritin-iron metabolism and the potential of lysosomes and proteasomes as targets for these drugs. However, it is of considerable interest that anthracyclines accumulate in acidic vacuoles such as lysosomes (Hurwitz et al., 1997) and vesicles of the Golgi apparatus (Klohs and Steinkampf, 1988). In their uncharged, hydrophobic state, anthracyclines diffuse across membranes, and within acidic compartments they become protonated and trapped (Hurwitz et al., 1997). In addition, early in vivo studies demonstrated that anthracyclines affect lysosomal morphology and enzyme activity (Singal et al., 1985). Furthermore, it has been shown in the mouse leukemia cell line L1210 that DOX has high affinity for the 20S subunit of the proteasome (Kiyomiya et al., 2001). Although interactions between anthracyclines and lysosomes or proteasomes have been described, precisely how these anticancer agents affect proteolytic systems remains to be further investigated. As shown in our current study, the activity of eight lysosomal enzymes was not affected by DOX. This observation suggested that the ferritin-^{59}Fe accumulation observed in the presence of this drug was not a general effect on lysosomal enzymes. However, DOX may inhibit other lysosomal proteases that are essential for ferritin turnover. Indeed, the precise identities of the proteases that degrade ferritin remain unknown.

The current study demonstrated that general depression of cellular protein synthesis inhibited ferritin degradation and the redistribution of metabolically useful iron (Figs. 7 and 8). The fact that DOX markedly and irreversibly inhibited protein synthesis (Fig. 9B) may be one mechanism by which it inhibits the renewal of essential proteolytic mechanisms. Certainly, some lysosomal enzymes such as sialidase have a short half-life of approximately 2.7 h (Vinogradova et al., 1998), and hence, continued protein synthesis is vital to renew lysosomal enzymatic activity. Other crucial molecules in the lysosomal pathway include the lysosome-associated membrane proteins and the membrane-bound transporter of cysteine (for review see Pillay et al., 2002). Inhibition of the synthesis of any of these essential molecules will disrupt the normal lysosomal degradation process. Moreover, recent studies have demonstrated that lysosomes are highly dynamic, capable of moving from the cell periphery to the perinuclear regions and vice versa (Radisky and Kaplan, 1998). Therefore, microtubules probably play a significant role in the stability and trafficking of lysosomes (Matteoni and Kreis, 1987) and could be a potential target for protein synthesis inhibition that can disrupt lysosomal activity.

There are more than 50 lysosomal hydrolases, and these can be classified into the aspartic, cysteine, and serine proteases (Pillay et al., 2002). Incubation of SK-Mel-28 melanoma cells with the aspartic protease inhibitor pepstatin A had little effect on ferritin-^{59}Fe accumulation (Fig. 10, A and B), suggesting that this class of enzymes is not primarily involved in ferritin-^{59}Fe mobilization. However, both E64d and leupeptin markedly increased ferritin-^{59}Fe accumulation, suggesting that cysteine and/or serine proteases may be responsible for ^{59}Fe mobilization from this molecule. In fact, it is possible that the localization of anthracyclines in lysosomes (Hurwitz et al., 1997) inhibits certain lysosomal enzymes (Singal et al., 1985), resulting in a marked accumulation of ferritin-iron.

Interestingly, the structurally distinct and widely used proteasome inhibitors MG132 and leupeptin also markedly prevented ferritin-^{59}Fe mobilization (Fig. 10, A and B). The reversible inhibitor, MG132, targets the chymotrypsin-like activity of the proteasome (Lee and Goldberg, 1998). However, it is not completely selective and has been demonstrated to also target certain lysosomal cysteine proteases and the calpains (Lee and Goldberg, 1998). Similarly, whereas lactacystin acts irreversibly and has higher specificity, it can also inhibit the lysosomal protease cathepsin A (Dick et al., 1996). Hence, it could be suggested that the accumulation of ferritin-^{59}Fe observed with the proteasome inhibitors MG132 and lactacystin were caused by the inhibition of lysosomal proteases. This could argue against a role for proteasomes in the degradation of ferritin-iron. Alternatively, because the ubiquitin-proteasome pathway also plays a major role in the selective degradation of intracellular proteins (Lee and Goldberg, 1998), it is not unreasonable to speculate that proteasomes may be involved in ferritin degradation. Indeed, various in vitro and cellular studies have demonstrated proteasome-mediated degradation of ferritin (Rudeck et al., 2000). It is also possible that the avid association of anthracyclines with the 20S proteasomal subunit (Kiyomiya et al., 2001) may prevent ferritin degradation. This would explain the marked accumulation of ferritin-^{59}Fe when cells were incubated with the proteasome inhibitors MG132 and lactacystin (Fig. 10, A and B).

It is relevant to discuss that the potent metabolic inhibitors cyanide, azide, and rotenone all prevented ^{59}Fe mobilization from ferritin in a manner similar to that of DOX (Fig. 6). These three agents have been shown to markedly reduce ATP levels in our previous studies over shorter or the same incubation period used in this investigation (Watts and Richardson, 2001; Kwok and Richardson, 2003), whereas DOX at the same concentration used in our experiments (i.e., 5–20 μM) did not (Kwok and Richardson, 2003). This suggests that the ferritin-^{59}Fe accumulation observed after incubation with DOX was not predominantly caused by a pronounced decrease in ATP levels and could be related to its other properties such as protein synthesis inhibition. However, the fact that marked metabolic depletion inhibits the ^{59}Fe-mobi-

lization process from ferritin indicates that this mechanism is energy-dependent.

In our previous study, we showed that the redox-cycling drugs menadione and paraquat also resulted in ferritin-^{59}Fe accumulation (Kwok and Richardson, 2003). This effect could be partially reversed by the cell-permeable glutathione peroxidase mimetic ebselen and the membrane-permeable superoxide dismutase mimetic MnTBAP (Kwok and Richardson, 2003). However, it is important to note that these agents were less effective at reversing ferritin-^{59}Fe accumulation induced by DOX (Kwok and Richardson, 2003). One possible explanation consistent with the current investigation is that the free radicals generated by these redox cycling agents may affect lysosomal function, as proposed in other studies (Persson et al., 2001).

In summary, the current study demonstrates that DOX inhibits ^{59}Fe mobilization from ferritin in the cytosol and SMM. We showed that inhibition of energy generation or protein synthesis inhibits the ferritin-^{59}Fe mobilization pathway. A variety of lysosomal enzyme inhibitors, proteasomal inhibitors, and lysosomotropic agents resulted in marked accumulation of ferritin-^{59}Fe that was comparable with that found using DOX. These data provide further evidence of a mechanism involving lysosomes in the degradation of ferritin for the release and redistribution of metabolically useful iron. The inhibition of iron redistribution from ferritin may have detrimental effects on vital iron-dependent processes in the cell. Considering that anthracyclines accumulate in lysosomes, it is possible that the lysosomal degradation pathway represents a potential target for anthracycline cytotoxicity.

Acknowledgments

We kindly thank the Department of Chemical Pathology, Women's and Children's Hospital, Adelaide, Australia, for measuring lysosomal enzyme activity using their established protocols.

References

Bienfait HF and Van der Briel ML (1980) Rapid mobilization of ferritin iron by ascorbate in the presence of oxygen. *Biochim Biophys Acta* **631:**507–510.
Bolann BJ and Ulvik RJ (1987) Release of iron from ferritin by xanthine oxidase. Role of the superoxide radical. *Biochem J* **243:**55–59.
Corsi B, Cozzi A, Arosio P, Drysdale J, Samtambrogio P, Campanella A, Biasiotto G, Albertini A, and Levi S (2002) Human mitochondrial ferritin expressed in HeLa cells incorporates iron and affects cellular iron metabolism. *J Biol Chem* **277:** 22430–22437.
Darnell G and Richardson DR (1999) The potential of iron chelators of the pyridoxal isonicotinoyl hydrazone class as effective antiproliferative agents III: the effect of the ligands on molecular targets involved in proliferation. *Blood* **94:**781–792.
Dick LR, Cruikshank AA, Greiner L, Melandri FD, Nunes SL, and Stein RL (1996) Mechanistic studies on the activation of the proteasome by lactacystin: a central role for clasto-lactacystin β-lactone. *J Biol Chem* **271:**7273–7276.
Funk F, Lenders JP, Crichton RR, and Schneider W (1985) Reductive mobilisation of ferritin iron. *Eur J Biochem* **152:**167–172.
Gianni L and Myers C (1992) The role of free radical formation in the cardiotoxicity of anthracycline, in *Cancer Treatment and the Heart* (Muggia FM, Green MD, and Speyer JL eds) pp 9–46, Johns Hopkins University Press, Baltimore.
Giljaard H (1980) *Genetic Metabolic Diseases: Early Diagnosis and Prenatal Analysis*, Elsevier/North Holland Biomedical Press, Amsterdam.
Harrison PM and Arosio P (1996) The ferritins: molecular properties, iron storage function and cellular regulation. *Biochim Biophys Acta* **1275:**161–203.
Hernandez-Yago J, Knecht E, Martinez-Ramon A, and Grisola S (1980) Autophagy of ferritin incorporated into the cytosol of Hela cells by liposomes. *Cell Tissue Res* **205:**303–309.
Hurwitz SJ, Terashima M, Mizunuma N, and Slapak CA (1997) Vesicular anthracycline accumulation in doxorubicin-selected U-937 cells: participation of lysosomes. *Blood* **89:**3745–3754.
Jin W, Takagi H, Pancorbo B, and Theil EC (2001) "Opening" the ferritin pore for iron release by mutation of conserved amino acids at interhelix and loop sites. *Biochemistry* **40:**7525–7532.
Kiyomiya K, Matsuo S, and Kurebe M (2001) Mechanism of specific nuclear transport of adriamycin: the mode of nuclear translocation of adriamycin-proteasome complex. *Cancer Res* **61:**2467–2471.
Klohs WD and Steinkampf RW (1988) The effect of lysosomotrophic agents and secretory inhibitors on anthracycline retention and activity in multiple drug-resistant cells. *Mol Pharmacol* **34:**180–185.
Knight CG and Barrett AJ (1976) Interaction of human cathepsin D with the inhibitor pepstatin. *Biochem J* **155:**117–125.
Kotamraju S, Chitambar CR, Kalivendi S, Joseph J, and Kalyanaraman B (2002) Transferrin receptor-dependent iron uptake is responsible for doxorubicin-mediated apoptosis in endothelial cells: role of oxidant-induced iron signaling in apoptosis. *J Biol Chem* **277:**17179–17187.
Kwok JC and Richardson DR (2002a) Anthracycline-mediated alterations in iron regulatory protein-RNA-binding activity: the iron and copper complexes of anthracyclines decrease RNA-binding activity. *Mol Pharmacol* **62:**888–900.
Kwok JC and Richardson DR (2002b) The iron metabolism of neoplastic cells: alterations that facilitate proliferation? *Crit Rev Haematol Oncol* **42:**65–78.
Kwok JC and Richardson DR (2003) Anthracyclines induce accumulation of iron in ferritin in myocardial and neoplastic cells: inhibition of the ferritin iron mobilization pathway. *Mol Pharmacol* **63:**849–861.
Lee DH and Goldberg AL (1998) Proteasome inhibitors: valuable new tools for cell biologists. *Trends Cell Biol* **8:**397–403.
Link G, Tirosh R, Pinson A, and Hershko C (1996) Role of iron in the potentiation of anthracycline cardiotoxicity: identification of heart cell mitochondria as a major site of iron-anthracycline interaction. *J Lab Clin Med* **127:**272–278.
Matteoni R and Kreis TE (1987) Translocation and clustering of endosomes and lysosomes depends on microtubules. *J Cell Biol* **105:**1253–1265.
McGowan EB, Becker E, and Detwiler TC (1989) Inhibition of calpain in intact platelets by the thiol protease inhibitor E-64d. *Biochem Biophys Res Commun* **158:**432–435.
Minotti G, Recalcati S, Mordente A, Liberi G, Calafiore AM, Mancuso C, Preziosi P, and Cairo G (1998) The secondary alcohol metabolite of doxorubicin irreversibly inactivates aconitase/iron regulatory protein-1 cytosolic fractions from human myocardium. *FASEB J* **12:**541–552.
Ohkuma S and Poole B (1978) Fluorescence probe measurement of the intralysosomal pH in living cells and the perturbation of pH by various agents. *Proc Natl Acad Sci USA* **75:**3327–3331.
Ohshita T, Nikawa T, Towatari T, and Katunuma N (1992) Effects of selective inhibition of cathepsin B and general inhibition of cysteine proteinases on lysosomal proteolysis in rat liver in vivo and in vitro. *Eur J Biochem* **209:**223–231.
Persson HL, Nilsson KJ, and Brunk UT (2001) Novel cellular defenses against iron and oxidation: ferritin and autophagocytosis preserve lysosomal stability in airway epithelium. *Redox Rep* **6:**57–63.
Pillay CS, Elliott E, and Dennison C (2002) Endolysosomal proteolysis and its regulation. *Biochem J* **363:**417–429.
Radisky DC and Kaplan J (1998) Iron in cytosolic ferritin can be recycled through lysosomal degradation in human fibroblasts. *Biochem J* **336:**201–205.
Richardson DR (1999) Role of ceruloplasmin and ascorbate in cellular iron release. *J Lab Clin Med* **134:**454–465.
Richardson DR and Baker E (1990) The uptake of iron and transferrin by the human melanoma cell. *Biochim Biophys Acta* **1053:**1–12.
Richardson DR and Milnes K (1997) The potential of iron chelators of the pyridoxal isonicotinoyl hydrazone class as effective anti-proliferative agents II: the mechanism of action of ligands derived from salicylaldehyde benzoyl hydrazone and 2-hydroxyl-1-napthylaldehyde benzoyl hydrazone. *Blood* **89:**3025–3038.
Rickwood D and Patel D (1995) Fractionation and analytical methods, in *Cell and Molecular Biology: Essential Data*, Wiley and Sons, Chichester, New York.
Roberts S and Bomford A (1988) Ferritin iron kinetics and protein turnover in K562 cells. *J Biol Chem* **263:**19181–19187.
Rudeck M, Volk T, Sitte N, and Grune T (2000) Ferritin oxidation in vitro: implication of iron release and degradation by the 20S proteasome. *IUBMB Life* **49:**451–456.
Singal PK, Segstro RJ, Singh RP, and Kutryk MJ (1985) Changes in lysosomal morphology and enzyme activities during the development of adriamycin-induced cardiomyopathy. *Can J Cardiol* **1:**139–147.
Speyer BE and Fielding J (1979) Ferritin as a cytosol iron transport intermediate in human reticulocytes. *J Br Haematol* **42:**255–267.
Vinogradova MV, Michaud L, Mezentsev AV, Lukong KE, El-Alfy M, Morales CR, Potier M, and Pshezhetsky AV (1998) Molecular mechanism of lysosomal sialidase deficiency in galactosialidosis involves its rapid degradation. *Biochem J* **330:**641–650.
Watts RN and Richardson DR (2001) Nitrogen monoxide (NO) and glucose. Unexpected links between energy metabolism and NO-mediated iron mobilization from cells. *J Biol Chem* **276:**4724–4732.
Zunino F, Pratesi G, and Perego P (2001) Role of the sugar moiety in the pharmacological activity of anthracyclines: development of a novel series of disaccharide analogs. *Biochem Pharmacol* **61:**933–938.

Address correspondence to: Dr. D.R. Richardson, Children's Cancer Institute Australia for Medical Research, Iron Metabolism and Chelation Program, P.O. Box 81, High Street, Randwick, Sydney, NSW 2031, Australia. E-mail: d.richardson@ccia.org.au